Journal of Chemistry

WILEY

RESEARCH ARTICLE OPEN ACCESS

Performance and Durability of Chemically Activated Lime-Based Cement Blended With Rice Husk Ash

Odiwuor Vincent Onyango | Fidelis Nekesa Samita | Martin W. Wetungu

Department of Chemistry and Biochemistry, University of Eldoret, P.O. Box 1125-30100, Eldoret, Kenya

Correspondence: Odiwuor Vincent Onyango (vincentodiwuor623@gmail.com)

Received: 4 May 2026 | **Revised:** 21 July 2026 | **Accepted:** 23 July 2026

Academic Editor: Sohini Basu Roy

Keywords: acid resistance | chemical activation | compressive strength | lime mortar | porosity | rice husk ash (RHA)

ABSTRACT

Lime–pozzolana binders offer a low-carbon alternative to conventional materials; however, their practical application is limited by slow strength development and insufficient durability, particularly under aggressive chemical environments. In addition, existing studies on chemical activation have largely focused on OPC-based systems, with limited attention to lime-based binders and their durability performance. This study investigates the effect of chemical activation on the performance and durability of lime–rice husk ash (RHA) mortars. The objective was to evaluate how sodium hydroxide (NaOH) and sodium sulfate (Na_2SO_4) influence compressive strength, porosity, and resistance to sulfuric acid attack of lime mortars. Physicochemical characterization confirmed that the RHA contained 94.95% SiO_2 with high amorphous content and strong pozzolanic reactivity (> 60% conductivity loss). Results showed that RHA incorporation improved lime mortar performance, while chemical activation significantly enhanced these properties. NaOH activation increased compressive strength by 132%, compared to 53% for Na_2SO_4, relative to the non-activated system. Porosity decreased progressively across the systems, with the lowest values observed in NaOH-activated mortars. Under acid exposure, all RHA-containing mortars outperformed pure lime, which disintegrated completely. Strength and mass losses were lower in activated systems, particularly with NaOH. Deterioration was more severe in 3% H_2SO_4 than in a 0.5% solution. The findings indicate that chemical activation improves the short-term performance of lime–RHA mortars, although reaction products were not directly quantified. These results highlight the potential of chemically activated lime–RHA mortars as sustainable construction materials, particularly in resource-constrained regions.

1 | Introduction

Ordinary Portland cement (OPC) remains the dominant binder in the global construction industry [1]. However, its production is both resource- and energy-intensive, contributing significantly to environmental degradation. Cement manufacturing is estimated to contribute approximately 5%–10% of global CO_2 emissions, making it a significant driver of climate change [2, 3]. Furthermore, the high energy demand associated with OPC production results in elevated costs, limiting its affordability, particularly for low-income populations in developing countries [4]. As a result, the construction sector is under growing pressure to adopt more sustainable and cost-effective alternatives to conventional OPC [5].

One widely adopted strategy to mitigate these challenges involves blending OPC with pozzolanic materials. This strategy reduces clinker content and lowers associated CO_2 emissions [4, 6]. While this approach offers incremental environmental benefits, more substantial reductions in carbon footprint can be achieved through the use of lime–pozzolana binder systems. Lime-based mortars are widely used in sustainable construction and in the rehabilitation of historic masonry, particularly in textile-reinforced mortar and composite-reinforced mortar systems

[7]. Unlike OPC-based materials, these systems eliminate the need for energy-intensive clinker production and are better suited for incorporating locally available resources, including agricultural residues [8]. Consequently, lime-based binders provide a viable pathway to address both environmental concerns and economic constraints in developing regions [9, 10].

The utilization of agricultural and industrial wastes as alternative construction materials has gained increasing attention as a sustainable waste management strategy [11]. Among these, rice husk ash (RHA), a by-product of rice processing, is particularly promising. Large quantities of rice husks are often disposed of through open burning, leading to environmental pollution despite their high silica content [12]. Although the resulting ash is typically considered nonbeneficial in its raw form, its conversion into a reactive pozzolanic material offers significant potential for sustainable construction applications [13].

RHA is especially attractive due to its high amorphous silica content, which imparts excellent pozzolanic reactivity. While it has traditionally been used as a supplementary cementitious material (SCM) in OPC systems, its role in lime-based binders is equally important. Recent studies [13–17] have shown that RHA enhances strength development through secondary reactions that form calcium silicate hydrate (C–S–H) gels. The formation of a dense C–S–H matrix reduces permeability and limits the ingress of aggressive species such as sulfates and chlorides, thereby improving durability. Additionally, this refined microstructure enhances resistance to acid attack by restricting the penetration of hydrogen ions into the binder matrix [18, 19].

Despite these advantages, lime-pozzolana systems are hindered by slow early-age strength development and relatively low durability, which limit their broader application [20]. This behavior is primarily attributed to the low solubility of silica at ambient temperatures and the inherently slow kinetics of the pozzolanic reaction between calcium hydroxide and reactive silica [21]. Consequently, the formation of strength-bearing C–S–H phases is delayed compared to the rapid hydration processes observed in OPC systems [22]. Unlike OPC hydration, which proceeds rapidly through hydraulic reactions, lime–pozzolana systems rely on gradual, pH-dependent dissolution processes that may take weeks to develop significant mechanical strength [23]. These limitations are further exacerbated under aggressive environmental conditions, such as sulfate and acid exposure, where inadequate resistance can lead to accelerated deterioration [19]. Therefore, improving both the strength development and durability of lime-based systems remains a key research priority.

To overcome these limitations, chemical activation has been proposed as an effective strategy to accelerate reaction kinetics and enhance binder performance. The use of alkaline and sulfate-based activators has shown promise in improving pozzolanic reactivity and strength development [14, 24–26]. However, it is important to note that most existing studies on chemical activation have predominantly focused on OPC-based systems, with comparatively limited investigation into lime-based binders. Moreover, prior research has largely emphasized mechanical performance, often overlooking critical durability aspects such as resistance to acid attack. As a result, there remains a significant research gap concerning the combined influence of chemical activators on both strength and durability in lime–pozzolana systems under controlled conditions.

In response to these gaps, the present study investigates the performance and durability of chemically activated lime–RHA mortars using sodium hydroxide and sodium sulfate as activators. The study focuses on evaluating compressive strength, porosity, and resistance to sulfuric acid attack after 28 days of ambient curing. The main objective of this study is to assess the effect of sodium hydroxide and sodium sulfate activation on the mechanical and durability properties of lime–RHA mortars. It is hypothesized that chemical activation will enhance the dissolution of amorphous silica and promote the formation of additional cementitious phases, leading to improved strength, reduced porosity, and enhanced resistance to aggressive chemical environments.

The proposed approach is expected to refine the pore structure and improve matrix densification without relying on high-energy processing or excessive activator concentrations. Unlike previous studies that primarily focus on OPC systems or isolated performance parameters, this work provides a comprehensive evaluation of chemical activation in lime-based binders. By optimizing the balance between calcium hydroxide and reactive silica, the study contributes to the advancement of sustainable, durable, and low-carbon construction materials based on locally available resources.

2 | Materials and Methods

2.1 | Materials

This study employed four key materials: RHA, hydrated lime (HL), river sand, and chemical activators. Rice husks were sourced from a processing facility in Homa Bay town, Kenya, where they are generated as a by-product of the milling process. A commercially available HL, conforming to IS 6932:1973 [27], was used. The river sand satisfied the requirements of IS 383:1970 [28], with all particles passing a 5 mm sieve, and it exhibited a specific gravity of 2.69 and a fineness modulus of 3.39. Additionally, sodium hydroxide and sodium sulfate were incorporated as chemical activators to enhance the reactivity of the binder system. HL, sodium hydroxide, and sodium sulfate were procured from Jackitos Enterprises Limited, Nairobi, Kenya. The HL was supplied as a powder with a stated purity of 98%, whereas NaOH and Na_2SO_4 were supplied in pellet and powder forms with purities of 97% and 99%, respectively.

2.2 | Methods

2.2.1 | Sample Preparation

The production of high-quality RHA requires an effective pretreatment stage, beginning with thorough cleaning of the raw rice husks. Husks collected from mills or farms typically contain impurities and foreign matter that must be removed to prevent deterioration of the ash quality and its performance in subsequent applications [29]. In this study, the husks were first subjected to an airstream to remove lighter contaminants such as dust, chaff, and fine particles. They were then washed with water to eliminate adhered dirt and soluble impurities, after which the washing liquid was filtered to recover the cleaned husks. Following cleaning, drying was carried out as a crucial step to reduce the moisture content to a suitable level for further processing [30]. The cleaned rice husks were oven-dried at 105°C for 24 h.

Adequate drying after cleaning is essential, as it limits the risk of microbial growth, improves the efficiency of subsequent thermal treatment, and contributes to the production of high-quality RHA [31].

2.2.2 | Combustion of Rice Husks

The cleaned rice husks were subsequently calcined at 600°C for 2 h in an air atmosphere using a muffle furnace (model OSK 9540-MK-SP 38351) to produce RHA. A controlled heating rate of approximately 10°C/min was maintained throughout the heating process. After calcination, the ash was allowed to cool naturally inside the furnace to room temperature over a period of 24 h. To enhance the fineness and pozzolanic reactivity, the resulting ash was then subjected to mechanical grinding in a laboratory-scale ball mill operated at a constant speed of 300 rpm for 30 min. This controlled milling process produced a fine and homogeneous powder, with approximately 95% of the particles smaller than 75 μm, thereby promoting uniform dispersion in the mortar mixes.

2.2.3 | Physical and Chemical Analysis

X-ray fluorescence spectroscopy (XRFS) was employed for chemical characterization using a sequential X-ray spectrophotometer (model PW4025), and the results were reported as oxide percentages. Loss on ignition (LOI) was determined to evaluate the amount of unburnt carbon and volatile components present in the RHA. For HL, the LOI was also considered an indicator of the degree of hydroxylation and carbonation. Approximately 1.0 ± 0.05 g of the sample was placed in a covered porcelain crucible and heated in an electric muffle furnace at 950°C ± 25°C for 1 h. After heating, the crucible was transferred to a desiccator and allowed to cool to room temperature to avoid moisture uptake before weighing. The LOI was then calculated as the percentage difference between the initial sample mass and the remaining mass after ignition. X-ray diffraction (XRD) and Fourier transform infrared (FTIR) spectroscopy were employed to characterize the mineralogical composition and identify the functional group bands of the RHA. The XRD analysis was carried out using a diffractometer equipped with Cu Kα radiation, operated at 40 kV and 20 mA, with a scanning rate of 3°/min over a 2θ range of 5°–70°. FTIR measurements were conducted using a spectrophotometer operating in attenuated total reflectance (ATR) mode with a resolution of 4 cm^{-1} within the spectral range of 4000–400 cm^{-1}. The specific surface area of RHA was determined using Brunauer–Emmett–Teller (BET) analysis using nitrogen (N_2) adsorption. The composition of RHA and HL used in this study is given in Table 1.

2.2.4 | Pozzolanic Activity by Electrical Conductivity (EC) Test

This test was done to assess the suitability and expected performance of RHA before incorporating it into mix designs. The test was conducted in accordance with the method described by Musyimi et al. [32]. Initially, 200 mL of distilled water was placed in a 500-mL glass beaker and heated to 40°C ± 1°C on a hot magnetic plate. Calcium hydroxide was then added gradually until a saturated solution was achieved, after which the mixture was stirred for 2 min using a magnetic stirrer. The initial EC of the saturated solution (EC_0) was measured using a conductivity meter. Subsequently, 5.0 g of the pozzolanic sample was introduced into the solution maintained at 40°C ± 1°C, and the mixture was continuously stirred for an additional 2 min. EC readings (EC_t) were then taken at 30 min intervals over a duration of 3 h. The pozzolanic activity was evaluated based on the change in EC, calculated as the difference between the conductivity of the saturated calcium hydroxide solution and that of the pozzolana-containing solution ($EC_0 - EC_t$). All tests were performed in triplicate for each pozzolanic sample, and the average values were reported.

2.2.5 | Mix Proportions

The mortar mixes were prepared using HL as the main binder, with RHA incorporated as a supplementary pozzolanic material. In the blended formulations, RHA replaced 50% of the lime by mass, producing a binary binder with an equal proportion of HL and RHA (1:1). The 50% RHA replacement level was selected based on previous studies demonstrating effective performance of lime–pozzolana binders at a 1:1 lime-to-pozzolana ratio [33, 34]. This proportion provides a favorable balance between the calcium hydroxide supplied by HL and the reactive amorphous silica present in RHA, thereby enhancing pozzolanic reactions and the formation of cementitious products. Furthermore, based on the oxide compositions of the raw materials in Table 1, a 50:50 mass blend of HL and RHA corresponds to a Ca:Si molar ratio of approximately 0.85:1. This intentionally silica-rich composition promotes near-complete consumption of $Ca(OH)_2$ while retaining sufficient reactive silica to sustain pozzolanic reactions throughout the curing period. A control mix containing 100% HL (L100) was also produced for comparison. All mortar specimens were proportioned with a constant binder-to-fine aggregate ratio of 1:3 by mass, consisting of 450 g of binder and 1350 g of standard sand. To maintain uniform workability across all mixtures, a liquid-to-binder (L/B) ratio of 0.55 was adopted. The full mix compositions, including the designations for both water-based and chemically activated systems, are presented in Table 2.

2.2.6 | Mixing Casting and Curing

Mortar mixing and curing were carried out in accordance with KS EAS 148–1:2000 [35], with slight adjustments to suit the lime–pozzolana system. The binder comprised a 1:1 mass ratio of HL and RHA, designated as LR50, while a mix containing 100% HL (L100) was used as the control. To maintain consistent workability across all mixes, a fixed L/B ratio of 0.55 was adopted. Depending on the formulation, the mixing liquid was either potable water, 0.5 M NaOH, or 0.5 M Na_2SO_4. The selected concentration of 0.5 M was based on preliminary trials (0.1–2.5 M), which identified it as optimal for enhancing chemical activation without adversely affecting matrix integrity. Sodium sulfate was used as a chemical activator based on previous studies demonstrating its effectiveness in sulfate-activated cementitious systems. Because the RHA contained only 0.50 wt.% Al_2O_3, Na_2SO_4 was employed to promote the dissolution of reactive amorphous silica and enhance the pozzolanic reaction between silica and calcium hydroxide in the lime–RHA binder [18, 26]. Mixing was conducted using a PANLab Analytica mixer. Initially, the dry binder and sand (450 g binder to 1350 g standard sand) were blended for 1 min to achieve uniformity. The designated liquid was then gradually introduced, and mixing

TABLE 1 | Chemical composition and physical properties of RHA and HL.

Composition	RHA	HL
SiO_2	94.95 ± 0.02	—
Al_2O_3	0.50 ± 0.001	0.21 ± 0.01
Fe_2O_3	0.19 ± 0.002	—
CaO	2.39 ± 0.02	87.44 ± 0.03
MgO	0.38 ± 0.001	1.34 ± 0.03
MnO	1.97 ± 0.09	—
Na_2O	0.25 ± 0.001	—
K_2O	1.09 ± 0.006	—
CdO	0.03 ± 0.001	—
LOI	2.96 ± 0.05	26.14 ± 0.02
BET (m^2/g)	50.2	—
Specific gravity	2.16	2.79

continued for an additional 4 min to obtain a consistent mortar. The fresh mix was cast into 40 × 40 × 160 mm prisms for compressive strength evaluation and 100 × 100 × 100 mm cubes for durability testing. Compaction was performed on a vibrating table for 2 min. After casting, specimens were labeled according to their mix type (LR50–H_2O, LR50–NaOH, and LR50–Na_2SO_4). To minimize moisture loss, the molds were covered with impermeable polyethylene sheets and stored at 22°C ± 2°C with relative humidity above 90% for 24 ± 0.5 h. Once demolded, the specimens were cured under ambient air conditions for 28 days. This curing approach was intentionally adopted to promote atmospheric carbonation, which is critical for strength development in lime-based systems. During curing, the laboratory environment was maintained at 23°C ± 3°C and an average relative humidity of 90% ± 5%, with specimens arranged to allow uniform exposure to CO_2.

2.2.7 | Compressive Strength

The compressive strength of the lime–RHA mortars was evaluated after 28 days of curing in accordance with KS EAS 148-1: 2000 [35]. Tests were conducted using a calibrated automatic compression testing machine (Model SSC-546). For consistency, the 40 × 40 × 160 mm prisms were loaded at a constant rate of 2400 ± 200 N/s until failure, as prescribed by the equipment manual and relevant standards. To ensure accuracy and reproducibility, the reported compressive strength for each mix was taken as the average of three specimens. The effectiveness of the chemical activators was assessed by determining the percentage variation in compressive strength (ΔC) at 28 days, calculated using Equation (1):

$$\Delta C = \frac{C_{act} - CH_2O}{CH_2O} \times 100, \quad (1)$$

where ΔC denotes the percentage change in compressive strength (%), C_{act} represents the compressive strength of chemically activated mortars (LR50–0.5 M NaOH or LR50–0.5 M Na_2SO_4) at 28 days, and CH_2O corresponds to the compressive strength of nonactivated mortar (LR50–H_2O) at the same curing age (MPa).

2.2.8 | Porosity

The effective porosity of the mortar specimens was evaluated at 28 days using 40 × 40 × 160 mm prisms, based on the water displacement technique. Initially, the specimens were oven-dried at 105°C ± 5°C until a constant mass was attained, defined as a variation of less than 0.1% over a 24-h interval. The dried samples were then submerged in deionized water for 24 h to ensure full saturation. While suspended in water, their apparent mass (W_c) was measured. After removal, excess surface water was gently wiped off using a damp cloth to achieve the saturated surface-dry (SSD) condition, and the corresponding mass in air t (W_a) was recorded immediately. The oven-dry mass is denoted as W_b. The effective porosity (P) was computed using Equation (2):

$$P = \frac{W_a - W_b}{W_a - W_c} \times 100. \quad (2)$$

2.2.9 | Resistance to Sulfuric Acid Attack

The chemical durability of lime–RHA mortars was assessed following ASTM C267:1997 [36], with slight modifications in specimen configuration. Instead of standard cubes, mortar prisms of dimensions 40 × 40 × 160 mm were employed. After the initial 28-day air-curing period, the specimens were split into two groups and immersed in sulfuric acid solutions of 0.5% and 3.0% by volume under controlled laboratory conditions at 23°C ± 1°C. This two-level concentration method was used to assess and compare the system's durability under both mild and highly aggressive acidic conditions. To preserve a stable corrosive environment and minimize acid neutralization by the alkaline constituents of the mortar, the acid solution was replaced on a weekly basis, ensuring consistent pH throughout the exposure period. At the end of the immersion duration, the specimens were retrieved, rinsed with tap water, and lightly cleaned using a soft nylon brush to remove loosely adhered corrosion products and surface deposits, enabling evaluation of the intact core material. Prior to testing, the specimens were air-dried for 3 h under laboratory conditions. The final mass and residual compressive strength were then determined. The residual weight retention (R_w) and residual compressive strength (R_s) were computed using Equations (3) and (4), respectively:

TABLE 2 | Characteristics of the binder mixtures.

Mix ID	% composition by weight Lime (%)	Mixture RHA (%)	Formulations Binder–liquid system
LR50	50	50	LR50–H_2O LR50–0.5 M NaOH LR50–0.5 M Na_2SO_4
L100	100	0	L100–H_2O

$$R_w = \frac{W_a - W_s}{W_a} \times 100, \quad (3)$$

$$R_s = \frac{C_i - C_t}{C_i} \times 100, \quad (4)$$

where W_a is the initial mass before acid exposure (g), W_s is the mass after acid exposure (g), C_i is the compressive strength at 28 days prior to immersion (MPa), and C_t is the compressive strength after 28 days of acid exposure (MPa). For each mix, the reported values represent the average of three replicate measurements.

3 | Results and Discussion

3.1 | Physical and Chemical Analysis

The composition of RHA and HL used in this study is given in Table 1.

The RHA sample shows very high SiO_2 content and very low Al_2O_3, Fe_2O_3, and CaO. This confirms that it is a highly siliceous pozzolan. Recent studies report that RHA is dominated by amorphous silica, with minor oxides such as CaO, MgO, K_2O, and Fe_2O_3 [17, 31, 37]. The silica content in this study exceeds the commonly reported 80%–90% range for well-burnt RHA [38]. This suggests high purity and effective calcination. High silica content enhances pozzolanic reactivity because silica reacts with calcium hydroxide to form C–S–H, the main strength-giving phase [39]. Table 1 indicates that the combined content of SiO_2, Al_2O_3, and Fe_2O_3 exceeds 70%, meeting the chemical composition requirement for Class N pozzolans specified in ASTM C618:2015 [40]. However, the pozzolanic behavior of the RHA in this study is not inferred from chemical composition alone. It is further supported by XRD results, which show the predominance of amorphous silica, and by the significant reduction in EC during testing, indicating active consumption of calcium ions through pozzolanic reactions [41].

HL shows very high CaO content, confirming it as a calcium-rich activator. This agrees with studies reporting CaO contents above 85% in HL [16, 21]. The combination of high silica in RHA and high CaO in HL indicates strong potential for pozzolanic reactions [17]. The low CaO content in RHA confirms that it is not self-cementing and requires an external calcium source. Minor oxides such as K_2O and Na_2O are typical of plant ashes. They can affect alkali reactivity and silicate hydrate formation. These alkalis also influence the pH, which controls hydrate stability. The alkali content of RHA remains below the 1.5% limit set by KS EAS 18-1:2017 [42].

LOI is commonly used to assess the amount of residual carbon and volatile constituents in pozzolanic materials. The low LOI recorded for RHA suggests efficient combustion during production and a low level of unburnt carbon [43]. In contrast, elevated LOI values in RHA are often linked to incomplete burning, which can increase water demand, weaken particle interactions, and adversely affect strength development [44]. For HL, however, LOI has a different significance. The relatively high LOI value of 26.14% is characteristic of HL and should not be interpreted as evidence of unburnt carbon. Instead, the mass loss is mainly attributed to the thermal decomposition of $Ca(OH)_2$ into calcium oxide (CaO), accompanied by the release of chemically bound water. Additional weight loss may arise from the decomposition of small quantities of calcium carbonate ($CaCO_3$) formed through carbonation during storage, together with minor moisture loss resulting from the hygroscopic nature of HL. Therefore, unlike RHA, the LOI of HL primarily reflects its degree of hydroxylation and carbonation rather than the presence of residual carbon.

The BET surface area of 50.2 m^2/g is relatively high. This indicates a fine and porous structure. Similar findings show that high surface area enhances reactivity and filler effects [4, 12]. High surface area also increases water demand for workability. A high surface area of RHA promotes faster dissolution and provides nucleation sites for hydrate formation, while HL supplies Ca^{2+} ions [45]. The specific gravity of RHA is lower than that of HL. This is typical and contributes to lighter and more volumetrically efficient mortars [14].

3.2 | XRD Analysis

The XRD diffraction peaks of RHA are revealed in Figure 1.

The XRD pattern of RHA shows a profile typical of highly reactive amorphous silica. The diffractogram is dominated by a broad hump between $2\theta \approx 15°$ and 30°, with maximum intensity around 20°–22°. This feature indicates the absence of long-range crystalline order. The lack of sharp peaks across the scan confirms that the material is largely noncrystalline. Such patterns are widely associated with reactive pozzolanic RHA. Amorphous silica is more reactive than crystalline forms. It dissolves readily in alkaline media and reacts with calcium hydroxide to form calcium silicate hydrate (C–S–H), which governs strength development in lime–pozzolana systems [46]. Similar observations show that amorphous RHA enhances compressive strength and durability [16, 37].

The absence of sharp crystalline peaks also reflects efficient calcination. The lack of quartz or cristobalite peaks suggests that the burning temperature was well controlled. This prevented the conversion of amorphous silica into crystalline phases. This is important because crystallization reduces reactivity and limits strength development [45]. Studies indicate that calcination within 500°C–700°C preserves the amorphous structure and improves performance [47, 48]. The diffuse nature of the pattern further suggests a high specific surface area, which promotes dissolution and reaction kinetics [15]. Crystalline impurities often behave as inert fillers or interfere with hydration [16]. The nearly featureless region beyond 30° suggests minimal interference from such phases. This supports reliable performance in practical applications. The XRD results also highlight the synergy between RHA and HL. HL supplies $Ca(OH)_2$, while amorphous silica in RHA acts as the reactive phase. This interaction forms C–S–H and strengthens the matrix. Without amorphous silica, lime remains weak and prone to leaching. Without lime, RHA cannot form binding phases. Therefore, the amorphous structure observed in the XRD pattern is critical to the effectiveness of the binder system [45, 49].

3.3 | Pozzolanic Activity of RHA

Figure 2 illustrates the results of the pozzolanicity test of RHA, expressed as the percentage loss in conductivity over time.

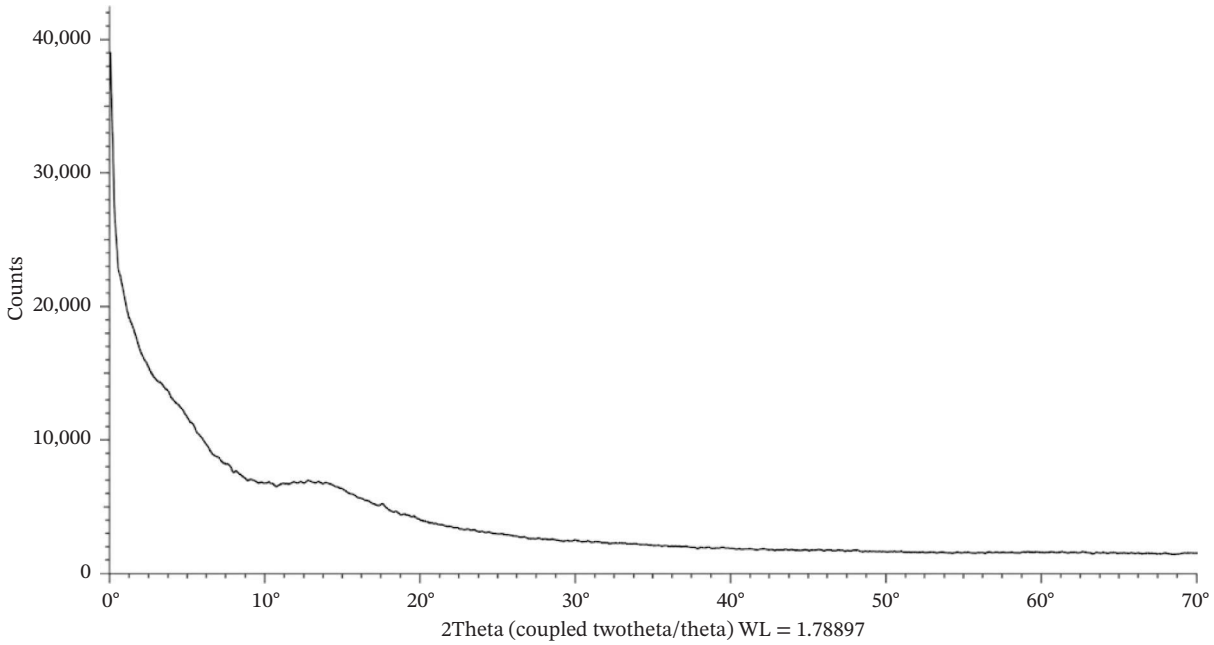

FIGURE 1 | XRD pattern of RHA sample.

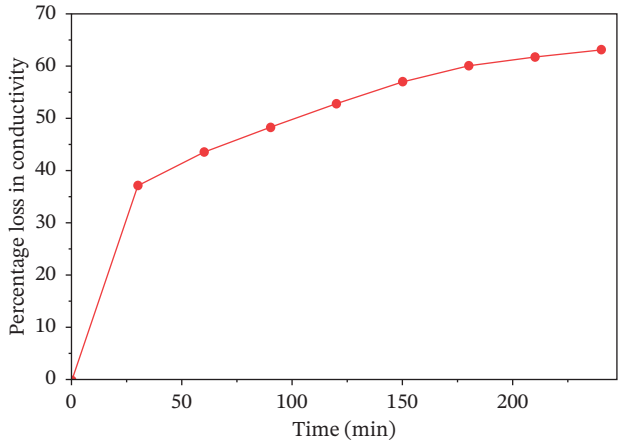

FIGURE 2 | Percentage loss in conductivity of the RHA sample.

The EC curve of the RHA–lime system shows a sharp conductivity loss within the first 30 min, followed by a gradual approach to a plateau at 240 min. This behavior is typical of a highly reactive pozzolan. It reflects the interaction between dissolved silica from RHA and Ca^{2+} ions in solution [50]. The trend indicates two kinetic regimes: an early rapid stage and a later diffusion-controlled stage. In the first 30 min, conductivity drops rapidly. This is due to the fast dissolution of amorphous silica and its reaction with Ca^{2+} to form early C–S–H [51]. The high surface area and presence of silanol groups accelerate this process. As ions are consumed, the EC decreases sharply [45]. Similar behavior has been reported for highly reactive pozzolans, where significant conductivity loss occurs within the first 30 min [32].

Between 30 and 120 min, the rate of conductivity loss decreases. This marks a transition to mixed kinetic control. The formation of C–S–H on particle surfaces begins to limit further silica dissolution [15]. The system becomes partly controlled by ion diffusion through the hydration layer. The C–S–H gel acts as a semipermeable barrier, slowing mass transport while allowing continued reaction [49]. From 120 to 240 min, the curve approaches a plateau. This indicates diffusion-controlled kinetics. Most reactive silica has already been consumed. The remaining core is less accessible due to encapsulation by hydration products. Ion transport through the C–S–H layer becomes the rate-limiting step [50]. The asymptotic trend suggests that further ion consumption is minimal. Similar patterns have been reported by Marangu [52].

The overall conductivity loss (> 60%) confirms strong pozzolanic activity of RHA. This agrees with the chemical composition and XRD/FTIR results of the RHA, which indicate dominant amorphous silica. The curve shape shows both high initial reactivity and sustained reaction over time. This suggests that RHA can contribute to early and long-term strength in lime systems. The consumption of $Ca(OH)_2$ reduces free lime, which is linked to durability issues such as leaching and carbonation [48]. The formation of C–S–H also refines pore structure and densifies the matrix, improving resistance to permeability and chemical attack [53].

While the conductivity-loss method offers a reliable indication of pozzolanic reactivity, monitoring the solution pH alongside conductivity measurements would provide further insight into the dissolution of silica and the consumption of calcium hydroxide during the reaction process. Although pH measurements were not included in the current study, their incorporation in future research would enable a more comprehensive assessment of the reaction mechanisms involved.

3.4 | FTIR Analysis

FTIR analysis was performed to provide supplementary evidence of the functional groups present in the RHA. The FTIR spectrum is provided in the Supporting Information (Figure S1) as supporting qualitative evidence. The spectrum exhibited absorption bands generally attributable to O–H stretching and bending vibrations, minor carbonate-related species, and Si–O–Si/Si–O–M

linkages in the low-wavenumber region, consistent with previously reported FTIR spectra of RHA [54–56]. However, moisture-related interference, likely arising from the instrument's optical components, broadened several absorption bands and limited the reliability of detailed peak interpretation. Consequently, the FTIR results are interpreted cautiously and are used only as supplementary qualitative evidence. The principal conclusions regarding the predominance of amorphous silica and the pozzolanic reactivity of the RHA are based primarily on the XRD and EC analyses, which provide more robust experimental support.

3.5 | Compressive Strength at 28th Day of Curing

The compressive test results are given in Figure 3.

The compressive strength results in Figure 3 show a clear increasing trend across the binder systems. Pure lime mortar ($L100–H_2O$) records the lowest strength. This is expected of pure lime mortars. Lime hardens mainly through carbonation, where calcium hydroxide reacts slowly with atmospheric CO_2 to form calcium carbonate. The process is diffusion-controlled and progresses from the surface inward [57]. At early ages, the reaction remains incomplete, and hence there is little formation of hydraulic phases such as C–S–H. As a result, particle bonding is weak and load transfer is limited, leading to low strength [16]. Similar behavior has been widely reported for nonhydraulic lime mortars [8, 58, 59].

The $LR50–H_2O$ system shows a clear strength improvement over pure lime. This improvement is due to the pozzolanic reactivity of RHA. The amorphous silica in RHA reacts with calcium hydroxide in the presence of water to form C–S–H [57]. These products enhance bonding and improve strength. The high surface area of RHA further supports this reaction [39]. However, the strength remains moderate. This is because the reaction rate is relatively slow under normal mixing conditions, and silica dissolution is limited by the pore solution chemistry. Similar gradual strength development has been reported in lime–RHA systems [16, 17].

The chemically activated systems show much higher strength than $LR50–H_2O$. The LR50–0.5 M Na_2SO_4 system shows about a 53% increase in compressive strength, while LR50–0.5 M NaOH shows about a 132% increase. These improvements arise from accelerated pozzolanic reactions [26, 27]. The activators enhance silica dissolution. This increases the interaction between dissolved silica and calcium ions [11]. As a result, the formation of cementitious products is accelerated. In contrast, the lower strength of $LR50–H_2O$ reflects the presence of unreacted pozzolana due to the absence of activation. Similar trends have been reported in activated lime–pozzolan systems [48, 60]. The principal pozzolanic reaction is presented by Equation (5).

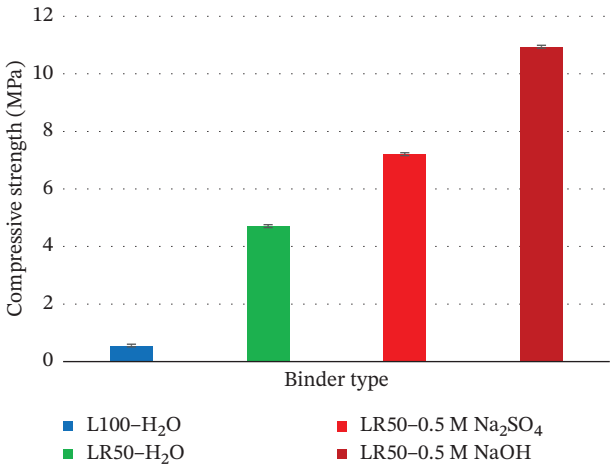

FIGURE 3 | Compressive strength of different lime mortars.

$$2SiO_2 + 3Ca(OH)_2 + 5H_2O \longrightarrow 3CaO.2SiO_2.8H_2O \quad (5)$$

$$Na_2SO_4 \longrightarrow 2Na^+ + SO_4^{2-} \quad (6)$$

The LR50–0.5 M Na_2SO_4 mixture exhibited moderate strength development compared with the LR50–0.5 M NaOH mixture. Unlike NaOH, Na_2SO_4 does not directly produce a highly alkaline solution. However, in the presence of $Ca(OH)_2$, it can react to generate NaOH in situ, providing an indirect source of alkalinity that promotes the dissolution of reactive amorphous silica from the RHA [61]. Sodium sulfate dissociates in solution according to Equation (6), while the OH^- ions generated through the in situ reaction enhance silica dissolution, increasing the concentration of dissolved silicate species available for the pozzolanic reaction. Similarly, the dissolved sodium ions may facilitate the dissolution of amorphous silica present in the RHA [62]. This increases the concentration of reactive silicate species in the system. The increased availability of dissolved silicate species can subsequently react with $Ca(OH)_2$ supplied by HL, promoting the formation of C–S–H, which contributes to strength development [63, 64]. However, the formation of C–S–H was inferred from the mechanical performance and known reaction mechanisms of activated lime–pozzolana systems, as it was not directly quantified in the present study. Given the relatively low Al_2O_3 content of the RHA, the formation of sulfate-containing reaction products such as ettringite is expected to be limited. The observed strength improvement is therefore more plausibly attributed to enhanced dissolution of amorphous silica and subsequent formation of additional C–S–H.

The LR50–0.5 M NaOH system achieved the highest compressive strength among the mixes. The simultaneous presence of Na^+ and OH^- ions enhances the dissolution of amorphous silica in RHA, leading to a higher concentration of reactive silicate species in the pore solution [65]. These silicate species then react with $Ca(OH)_2$ released from HL to form additional C–S–H, resulting in improved mechanical performance [66]. Similar behavior is reported in alkali-activated systems, where strong alkalis produce rapid reactions and superior mechanical performance [26, 64, 67, 68]. While the increased alkalinity of NaOH contributes to silica dissolution according to literature [25, 26, 64], the strength improvement is more closely linked to the greater availability of dissolved silicates and their subsequent incorporation into C–S–H formation, as illustrated in Equations (7) and (8).

$$SiO_2 + 2NaOH \longrightarrow Na_2SiO_3 + H_2O \quad (7)$$

$$Na_2SiO_3 + Ca(OH)_2 + nH_2O \longrightarrow CaO{\cdot}SiO_2{\cdot}nH_2O + 2NaOH \quad (8)$$

It should be noted that the dissolved silica does not exist as a single discrete species such as Na_2SiO_3. Instead, ^{29}Si NMR studies have shown that aqueous silicate solutions comprise a dynamic mixture of monomeric, oligomeric, and polymeric silicate species, with the degree of polymerization increasing as the SiO_2/Na_2O ratio increases [62, 69]. Accordingly, Equation (7) is presented as a simplified representation of the dissolution process rather than a literal stoichiometric reaction. Because pore solution pH was not measured in the present study, the evolution of silicate speciation during curing could not be monitored directly. Therefore, the proposed mechanism should be regarded as consistent with, but not conclusively confirmed by, the observed mechanical performance.

A one-way analysis of variance (ANOVA) showed that the mortar formulation had a highly significant effect on compressive strength ($p < 0.001$). In addition, Tukey's HSD post hoc analysis revealed statistically significant differences ($p < 0.05$) between every pair of mortar mixtures. These findings confirm that both the incorporation of RHA and chemical activation had a significant positive influence on the mechanical performance of the lime-based mortars. All analyses were performed at a 95% confidence level.

3.6 | Porosity

Porosities of different mortars considered are given in Figure 4.

The porosity results show a clear decreasing trend across the binder systems. This trend reflects progressive reaction and pore refinement, leading to improved matrix densification. L100–H_2O exhibits the highest porosity. This is typical of pure lime mortars. Hardening occurs mainly through slow carbonation, with little or no hydraulic reaction [57]. As a result, spaces previously occupied by mixing water remain as pores after drying. This leads to a highly porous matrix [58]. The LR50–H_2O system shows reduced porosity compared to pure lime. This is due to the pozzolanic reaction of RHA [64]. Amorphous silica reacts with calcium hydroxide to form C–S–H. These products precipitate within voids and partially fill the pore structure. This creates a denser matrix than the control system [18].

Further reduction is observed in the chemically activated systems. LR50–0.5 M Na_2SO_4 shows lower porosity than LR50–H_2O, while LR50–0.5 M NaOH shows the lowest value. Chemical activators are known to accelerate pozzolanic reactions by altering the chemistry of the pore solution. This enhances the dissolution of reactive silica and promotes the formation of additional cementitious hydration products [25]. Although pore solution pH was not determined in this study, the observed decrease in porosity suggests a greater degree of pozzolanic reaction and improved matrix densification, consistent with findings reported for chemically activated lime–pozzolana systems. NaOH resulted in a more pronounced reduction in porosity. The combined presence of Na^+ and OH^- ions promotes the dissolution of amorphous silica, thereby increasing the concentration of dissolved silicate species in the pore solution. The greater availability of these reactive silicates enhances their reaction with calcium hydroxide released from HL, leading to increased formation of C–S–H. The resulting increase in hydration products can contribute to pore refinement and a denser microstructure. However, these mechanisms were not directly investigated in the present study and are therefore inferred from trends reported in the literature.

3.7 | Acid Attack Resistance

Figures 5 and 6 present the strength and weight loss, respectively, for different binders subjected to varying acid concentrations.

The results show a consistent trend in both weight loss and strength loss under acid exposure. Exposure of mortar specimens to acidic media generally leads to progressive degradation of the material. Acid attack primarily involves dissolution of calcium-bearing phases. Sulfuric acid reacts with calcium hydroxide and other calcium-based reaction products formed in the lime–pozzolana system. This reduces the alkalinity of the mortar and promotes dissolution of these cementitious compounds, resulting in deterioration reflected by losses in weight and compressive strength [18, 19]. Both parameters increase with acid concentration. The 3% H_2SO_4 solution causes significantly higher deterioration than the 0.5% solution. This is due to the higher availability of hydrogen ions, which accelerates the dissolution of calcium-bearing phases. More material is leached out within a shorter time, leading to greater mass loss and reduction in strength. In addition, sulfuric acid reacts with calcium compounds to form gypsum, which contributes to softening and weakening of the matrix. These processes progressively remove solid material and reduce the structural integrity of the mortar [70].

Among the RHA-containing mixes, LR50–H_2O shows the highest loss in both weight and strength. This indicates lower resistance to acid attack. The slow pozzolanic reaction in a nonactivated system may result in a higher amount of unreacted calcium hydroxide, which is highly susceptible to acid dissolution. The reaction leads to leaching and progressive weakening. Lime-rich systems are known to have poor acid resistance due to the instability of calcium hydroxide in acidic environments [71]. The relatively high porosity of the LR50–H_2O system likely facilitated the penetration of acidic solutions into the mortar matrix, accelerating deterioration and consequently reducing its resistance to acid attack. The chemically activated mortars show lower losses. This indicates improved resistance to acid attack. Similar improvements in acid resistance have been reported for activated lime–pozzolan systems [19, 64].

The improved acid resistance of activated systems is attributed principally to the lower effective porosity shown in Figure 4, rather than to bulk pH effects or sustained alkalinity buffering during acid exposure. The sodium species introduced by the activators promote the dissolution of amorphous silica from RHA, increasing the concentration of reactive silicate species in the system. Increased dissolution of reactive silica promoted the formation of additional C–S–H, leading to pore refinement and matrix densification. This explanation is consistent with the observed correlation between acid resistance, compressive strength, and porosity across all mortar mixtures. Nevertheless, the possible influence of residual alkali species retained within the hardened matrix cannot be discounted, as such species may have provided a degree of buffering against penetrating H^+ ions during acid exposure. Although the sulfuric acid solution was renewed weekly to maintain the aggressiveness of the exposure environment and prevent bulk solution neutralization, residual alkali content, pore solution composition, and alkali leaching

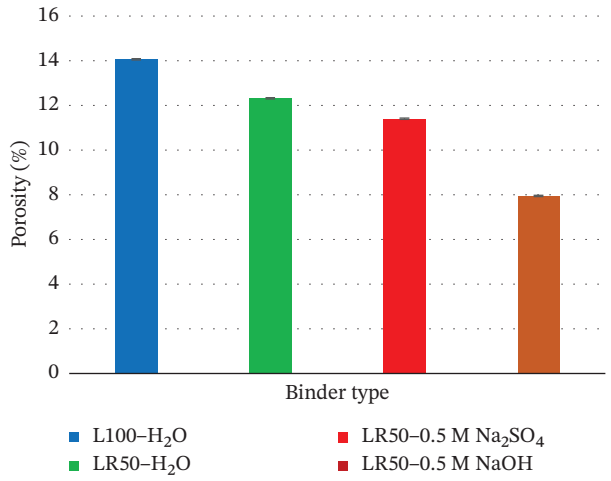

FIGURE 4 | Porosity of different lime mortars.

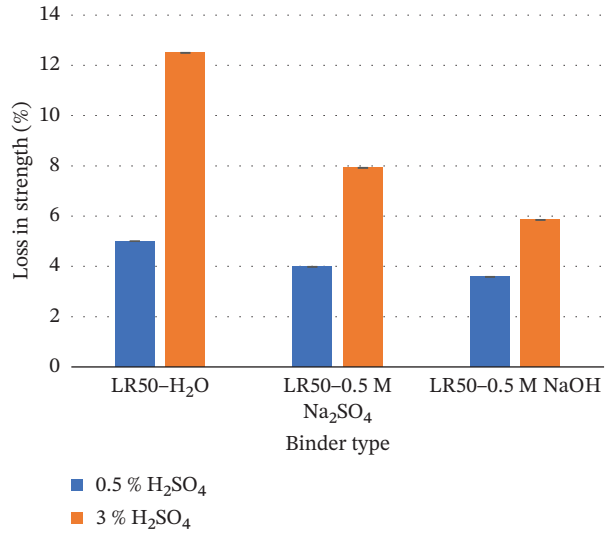

FIGURE 5 | Strength loss of different lime mortars.

were not evaluated. Therefore, the proposed mechanism should be regarded as a plausible interpretation based on the observed performance trends rather than a conclusion directly confirmed by experimental evidence.

Among the activated mortars, LR50–0.5 M NaOH exhibited the lowest deterioration, indicating the highest resistance to acid attack. LR50–0.5 M Na_2SO_4 demonstrated moderate performance, with degradation levels falling between those of the NaOH-activated and non-activated systems. The superior acid resistance of the NaOH-activated mortar can be attributed to the influence of NaOH on the relative solubility of $Ca(OH)_2$ and amorphous silica. Through the common-ion effect, excess dissolved Na^+ suppresses further dissolution of $Ca(OH)_2$ while enhancing the dissolution of amorphous silica from RHA [72]. The increased availability of dissolved silicate species promotes more extensive and rapid formation of C–S–H, leading to a denser microstructure and lower effective porosity. This refinement of the pore network limits the penetration and transport of H^+ ions into the mortar, slowing the deterioration process. This interpretation is consistent with the observed relationship between porosity, compressive strength, and acid resistance across all mortar systems investigated in this study.

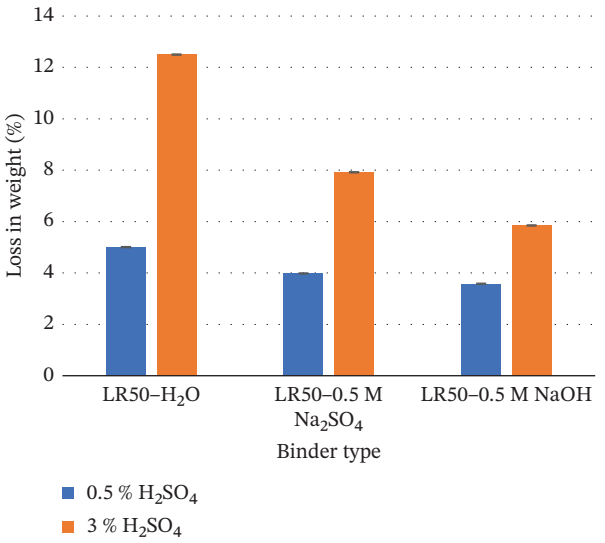

FIGURE 6 | Weight loss of different lime mortars.

Pure lime mortar disintegrated completely in acid. This is expected since it consists mainly of calcium hydroxide and calcium carbonate, both of which are highly reactive in acidic conditions. Calcium hydroxide dissolves rapidly, while calcium carbonate reacts to release CO_2 and form soluble salts. These reactions remove the binding phases entirely. The structure loses cohesion and collapses [7, 73]. The incorporation of RHA improves resistance by consuming calcium hydroxide and forming more stable binding products, which reduces susceptibility to acid attack [17]. Overall, resistance to acid attack improves in the order L100–H_2O (complete failure) < LR50–H_2O < LR50–0.5 M Na_2SO_4 < LR50–0.5 M NaOH. This trend reflects decreasing availability of acid-soluble phases and improved chemical stability of the binder system.

4 | Future Perspective

- Future studies should investigate a broader range of curing ages, RHA replacement levels, and NaOH and Na_2SO_4 concentrations, including their combined use, to establish optimum activation conditions for lime–RHA mortars. Such studies would provide greater insight into the relationships between activator dosage, hydration products, microstructural evolution, mechanical performance, and long-term durability.
- Further research should evaluate the effects of chemical activators in both RHA-containing and pure lime systems to distinguish their direct influence on lime hydration and acid resistance from their role in enhancing pozzolanic reactions. Simultaneous monitoring of pore solution pH, residual alkali content, and alkali leaching during immersion in deionized water would also help clarify the respective contributions of matrix densification and residual alkali species to durability.
- Advanced post-exposure characterization using techniques such as XRD, FTIR, TGA, and SEM should be undertaken to identify hydration and degradation products, confirm the formation of gypsum and other sulfate-bearing phases, and

evaluate changes in the microstructure following acid exposure. These investigations would provide direct evidence of the mechanisms governing strength development, acid resistance, and deterioration in chemically activated lime–RHA mortars.

5 | Conclusion

This study evaluated the performance of lime–RHA mortars through chemical activation using 0.5 M sodium hydroxide (NaOH) and 0.5 M sodium sulfate (Na_2SO_4) solutions. From the study, the following conclusions were made:

- RHA exhibited high silica content, predominantly amorphous silica, and measurable pozzolanic reactivity, indicating its suitability as a supplementary pozzolanic material in lime-based binder systems.
- Incorporation of RHA improved the compressive strength and sulfuric acid resistance of HL mortar compared with the unmodified lime mortar.
- Chemical activation further enhanced mortar performance, with NaOH producing greater improvements in compressive strength and sulfuric acid resistance than Na_2SO_4 under the conditions investigated.
- The observed improvements are consistent with enhanced pozzolanic reactions and a denser mortar matrix; however, these mechanisms were inferred from the experimental results and supporting literature rather than directly confirmed through microstructural characterization after exposure.
- The study demonstrated a feasible approach to improving the performance of lime-based mortars using locally available RHA and low-concentration chemical activators, offering a more sustainable alternative to conventional binders.
- The findings support the use of locally available RHA as a sustainable supporting information for producing more durable and lower-carbon lime-based binders, contributing to reduced reliance on OPC.

Author Contributions

Odiwuor Vincent Onyango: conceptualization, writing–original draft, writing–review and editing, and visualization.

Fidelis Nekesa Samita and Martin W. Wetungu: writing–review and editing.

Acknowledgments

This study was made possible through the support provided by several institutions during both the experimental phase and the preparation of this manuscript. The authors gratefully acknowledge these institutions for access to scholarly resources, library materials, laboratory facilities, and consumables, particularly the University of Eldoret and Eldoret National Polytechnic, Kenya.

Declaration of Generative AI and AI-Assisted Technologies in the Writing Process. During the preparation of this manuscript, the authors used AI-assisted software solely to improve the language, grammar, and readability of the text. The AI tool was not used to generate research data, perform analyses, interpret results, or formulate scientific conclusions. The authors critically reviewed and edited all AI-assisted outputs and accept full responsibility for the content of the manuscript.

Funding

This research did not receive any external funding.

Conflicts of Interest

The authors declare no conflicts of interest.

Data Availability Statement

The data used to support the findings of this study are available from the corresponding author upon request.

References

1. T. R. Naik, "Sustainability of Concrete Construction," *Practice Periodical on Structural Design and Construction* 13, no. 2 (2008): 98–103, https://doi.org/10.1061/(asce)1084-0680(2008)13:2(98).

2. A. Naqi and J. Jang, "Recent Progress in Green Cement Technology Utilizing Low-Carbon Emission Fuels and Raw Materials: A Review," *Sustainability* 11, no. 2 (2019): 537, https://doi.org/10.3390/su11020537.

3. O. E. Ige, O. A. Olanrewaju, K. J. Duffy, and C. Obiora, "A Review of the Effectiveness of Life Cycle Assessment for Gauging Environmental Impacts From Cement Production," *Journal of Cleaner Production* 324 (November 2021): 129213, https://doi.org/10.1016/j.jclepro.2021.129213.

4. J. M. Marangu, C. Muturia M'thiruaine, and M. Bediako, "Physico-chemical Properties of Hydrated Portland Cement Blended With Rice Husk Ash," *Journal of Chemistry* 2020 (2020): e5304745–10, https://doi.org/10.1155/2020/5304745.

5. U. Chandru, T. Vijay, A. Bahurudeen, and R. Senthilkumar, "Evaluating the Availability and Carbon Footprint of Agricultural Waste Ashes: A Strategy for Achieving Sustainable Cement Production in India," *Innovative Infrastructure Solutions* 9, no. 12 (November 2024): 482, https://doi.org/10.1007/s41062-024-01736-7.

6. F. N. Musyimi, J. M. Wachira, J. K. Thiong'o, and J. M. Marangu, "Performance of Ground Clay Brick Mortars in Simulated Chloride and Sulphate Media," *Journal of Engineering* 2019 (November 2019): 1–12, https://doi.org/10.1155/2019/6430868.

7. N. Azimi, K. Schollbach, D. V. Oliveira, T. D'Antino, and P. B. Lourenço, "Durability of Natural Hydraulic Lime–Pozzolan Mortars for TRM Strengthening Systems Under Acidic Aging: Linking Microstructural Degradation to Mechanical Performance via Chemo-Mechanical Modeling," *Construction and Building Materials* 500 (2025): 144244, https://doi.org/10.1016/j.conbuildmat.2025.144244.

8. M. Ramesh, M. Azenha, and P. B. Lourenço, "Mechanical Properties of Lime–Cement Masonry Mortars in Their Early Ages," *Materials and Structures* 52, no. 1 (2019): 13, https://doi.org/10.1617/s11527-019-1319-z.

9. K. J. Wołosz, K. Urbaniec, and N. Duić, "Sustainable Development of Energy, Water and Environment Systems (SDEWES)," *Sustainability* 13, no. 9 (April 2021): 4939, https://doi.org/10.3390/su13094939.

10. N. Marandi and S. Shirzad, "Sustainable Cement and Concrete Technologies: A Review of Materials and Processes for Carbon Reduction," *Innovative Infrastructure Solutions* 10, no. 9 (August 2025): 408, https://doi.org/10.1007/s41062-025-02213-5.

11. F. Ngui, N. Muhammed, F. M. Mutunga, J. M. Marangu, M. Otieno, and V. K. Mutai, "Strength and Durability Performance of Hybrid Alkaline Clay Brick Waste–Coconut Shell Ash Cement," *Journal of Sustainable Construction Materials and Technologies* 9, no. 4 (2024): 374–390, https://doi.org/10.47481/jscmt.1607846.

12. H. B. Dizaji, T. Zeng, I. Hartmann, et al., "Generation of High-Quality Biogenic Silica by Combustion of Rice Husk and Rice Straw Combined With Pre-and Post-Treatment Strategies—A Review," *Applied Sciences* 9, no. 6 (2019): 1083, https://doi.org/10.3390/app9061083.

13. J. R. Nayak, M. Gołaszewska, and J. Bochen, "Physical and Mechanical Performance of Mortar With Rice Husk Ash and Sugarcane Bagasse Ash as Partial Cement Replacement," *Materials* 18, no. 20 (2025): 4758, https://doi.org/10.3390/ma18204758.

14. E. E. Ambrose, O. R. Ogirigbo, T. B. Bello, and S. U. Akpando, "Compressive Strength, Density, and Setting Time of Concrete Blended With Rice Husk Ash," in *The 6th International Electronic Conference On Applied Sciences* (Benin, nigeria, 2026).

15. A. Shukla, K. Kishore, and N. Gupta, "Mechanical Properties of Cement Mortar With Lime & Rice Husk Ash," *IOP Conference Series: Materials Science and Engineering* 1116, no. 1 (2021): 012025.

16. R. Malathy, I.-M. Chung, S. H. Kim, M. Prabakaran, and R. Shanmugam, "Mechanical and Microstructural Properties of Composite Mortars With Lime, Silica Fume, and Rice Husk Ash," *Processes* 10, no. 7 (2022): 1424, https://doi.org/10.3390/pr10071424.

17. M. Doğruyol, "Characterization of Historic Mortars and the Effect of Rice Husk Ash (RHA) on Quicklime," *Case Studies in Construction Materials* 21 (2024): e03542, https://doi.org/10.1016/j.cscm.2024.e03542.

18. M. J. Mwiti, T. J. Karanja, and W. J. Muthengia, "Properties of Activated Blended Cement Containing High Content of Calcined Clay," *Heliyon* 4, no. 8 (2018): e00742, https://doi.org/10.1016/j.heliyon.2018.e00742.

19. T. A. Aiken, L. Gu, J. Kwasny, G. F. Huseien, D. McPolin, and W. Sha, "Acid Resistance of Alkali-Activated Binders: A Review of Performance, Mechanisms of Deterioration and Testing Procedures," *Construction and Building Materials* 342 (2022): 128057, https://doi.org/10.1016/j.conbuildmat.2022.128057.

20. R. Reis, A. Camões, and M. Ribeiro, "Hydrated Lime Treatment of Pozzolanic Mortars: Mechanical Performance and Accelerated Carbonation," *Sci* 8, no. 2 (2026): 45, https://doi.org/10.3390/sci8020045.

21. S. Ramanathan, L. R. Pestana, and P. Suraneni, "Reaction Kinetics of Supplementary Cementitious Materials in Reactivity Tests," *Cement* 8 (2022): 100022, https://doi.org/10.1016/j.cement.2022.100022.

22. A. B. Degefa, S. Park, B. Yang, and S. Park, "Predicting the Degree of Reaction of Supplementary Cementitious Materials in Hydrated Portland Cement," *Sustainability* 15, no. 21 (2023): 15471, https://doi.org/10.3390/su152115471.

23. C. Rodriguez-Navarro, T. Ilić, E. Ruiz-Agudo, and K. Elert, "Carbonation Mechanisms and Kinetics of Lime-based Binders: An Overview," *Cement and Concrete Research* 173 (2023): 107301, https://doi.org/10.1016/j.cemconres.2023.107301.

24. A. A. Tanjung, H. M. Ahmed, and H. A. M. Ahmed, "Enhancing the Activation of Saudi Natural Pozzolan Using Thermal, Mechanical, Chemical, and Hybrid Treatment Approaches," *Buildings* 15, no. 24 (2025): 4535, https://doi.org/10.3390/buildings15244535.

25. J. M. Marangu, J. K. Thiong'o, and J. M. Wachira, "Chloride Ingress in Chemically Activated Calcined Clay-Based Cement," *Journal of Chemistry* 2018, no. 2 (2018): 1–8, https://doi.org/10.1155/2018/1595230.

26. M. J. Mwiti, T. J. Karanja, and W. J. Muthengia, *Thermal Resistivity of Chemically Activated Calcined Clay-Based Cements* (RILEM Bookseries, 2017), 327–333.

27. Is6932, *Laboratory Tests on Building Lime* (New Delhi, India: Bureau of Indian Standards, 1973).

28. Is383, *Specification for Coarse and Fine Aggregates From Natural Sources for Concrete* (New Delhi, India: Bureau of Indian Standards, 1970).

29. H. R. Naik, T. Amin, and S. Sheraz Mahdi, *Post-Harvest Management and Value Addition of Food Crops* (Springer eBooks, 2022), 131–146.

30. A. Bazargan, T. Gebreegziabher, C.-W. Hui, and G. McKay, "The Effect of Alkali Treatment on Rice Husk Moisture Content and Drying Kinetics," *Biomass and Bioenergy* 70 (November 2014): 468–475, https://doi.org/10.1016/j.biombioe.2014.08.018.

31. S. Barbhuiya, B. B. Das, D. Adak, A. Rajput, and V. Katare, "Rice Husk Ash in Structural Concrete: Influence on Strength, Durability, and Sustainability," *Discover Concrete and Cement* 1, no. 1 (2025): 14, https://doi.org/10.1007/s44416-025-00013-9.

32. N. F. Musyimi, J. Karanja, M. Wachira, and M. Mulwa, "Pozzolanicity and Compressive Strength Performance of Kibwezi Bricks Based on Cement," *IOSR Journal of Applied Chemistry* 9, no. 2 (2016): 28–32.

33. S. Pavía and M. Aly, "Influence of Aggregate and Supplementary Cementitious Materials on the Properties of Hydrated Lime (CL90s) Mortars," *Materiales de Construcción* 66, no. 324 (November 2016): 104, https://doi.org/10.3989/mc.2016.01716.

34. L. P. B. Sales, A. F. da Nóbrega, A. C. V. da Nóbrega, R. de L. M. de C. Malheiro, M. S. de França, and P. Suraneni, "$CaCl_2$ as a Hardening Accelerator for Air Lime-Metakaolin Slurries: Effects of Two Different Types of Metakaolin on Kinetics, Rheology, and Microstructure," *Applied Clay Science* 292 (November 2026): 108302, https://doi.org/10.1016/j.clay.2026.108302.

35. *KS EAS 148:1, Kenya Standard Test Method for Determination of Cement Strength* (Nairobi, Kenya: Kenya Bureau of Standards, 2000).

36. Astm C267-97, *Standard Test Methods for Chemical Resistance of Mortars, Grouts, Monolithic Surfacings, and Polymer Concretes* (West Conshohocken, PA, USA: ASTM, 1997).

37. P. P. Kumar, H. S. Rao, and V. Giridhar, "A Study on Durability and Microstructural Analysis of High-Strength Concrete Utilizing Rice Husk Ash and Non-Biodegradable Polyethylene," *Discover Materials* 5, no. 1 (2025): 209, https://doi.org/10.1007/s43939-025-00267-x.

38. B. O. Okoya, D. Simeon, S. W. Mumenya, and S. O. Abuodha, "Characteristics of Kenyan Rice Husk Ash Produced Under Controlled Burning," *International Journal of Engineering Research and Technology* 10, no. 11 (2021).

39. H. Tural, I. Ince, B. Ozarisoy, and S. Derogar, "Investigating the Governing Factors Influencing the Pozzolanic Activity Through a Database Approach for the Development of Sustainable Cementitious Materials," *Construction and Building Materials* 411 (2024): 134253, https://doi.org/10.1016/j.conbuildmat.2023.134253.

40. Astm C618-15, *Standard Specification for Coal Fly Ash and Raw or Calcined Natural Pozzolan for Use in Concrete* (West Conshohocken, USA: American Society for Testing and Materials (ASTM), 2015).

41. S. A. Endale, W. Z. Taffese, D.-H. Vo, and M. D. Yehualaw, "Rice Husk Ash in Concrete," *Sustainability* 15, no. 1 (2022): 137, https://doi.org/10.3390/su15010137.

42. Ks Eas 18-1, *Kenya Standard Test Method for Oxides Specification of Hydraulic Cement* (Nairobi, Kenya: Kenya Bureau of Standards, 2017).

43. N. Chusilp, C. Jaturapitakkul, and K. Kiattikomol, "Effects of LOI of Ground Bagasse Ash on the Compressive Strength and Sulfate Resistance of Mortars," *Construction and Building Materials* 23, no. 12 (2009): 3523–3531, https://doi.org/10.1016/j.conbuildmat.2009.06.046.

44. H.-J. Chen, N.-H. Shih, C.-H. Wu, and S.-K. Lin, "Effects of the Loss on Ignition of Fly Ash on the Properties of High-Volume Fly Ash Concrete," *Sustainability* 11, no. 9 (May 2019): 2704, https://doi.org/10.3390/su11092704.

45. R. Walker and S. Pavía, "Physical Properties and Reactivity of Pozzolans, and Their Influence on the Properties of Lime–Pozzolan Pastes," *Materials and Structures* 44, no. 6 (2010): 1139–1150, https://doi.org/10.1617/s11527-010-9689-2.

46. P. Sargent, *Pozzolanic Reaction-an Overview* (ScienceDirect Topics, 2015).

47. A. U. Elinwa, "X-Ray and Microstructure of Rice Husk Ash-Admixed Concrete," *Exploratory Materials Science Research* 5, no. 2 (2023): 092–106.

48. D. O. Nduka, B. J. Olawuyi, E. O. Fagbenle, and B. G. Fonteboa, "Mechanical and Microstructural Properties of High-Performance Concrete Made With Rice Husk Ash Internally Cured With Superabsorbent Polymers," *Heliyon* 8, no. 9 (2022): e10502, https://doi.org/10.1016/j.heliyon.2022.e10502.

49. S. Velázquez, J. Monzó, M. Borrachero, and J. Payá, "Assessment of Pozzolanic Activity Using Methods Based on the Measurement of Electrical Conductivity of Suspensions of Portland Cement and Pozzolan," *Materials* 7, no. 11 (2014): 7533–7547, https://doi.org/10.3390/ma7117533.

50. I. V. Fernandes, D. J. C. Barbosa, C. F. G. Nascimento, M. D. Santos, M. Cartaxo, and A. A. M. Neto, "Assessment of the Pozzolanic Activity of Supplementary Cementitious Materials Through Electrical Conductivity: A Systematic Methodological Review With a Scientometric Approach," *Journal of Building Pathology and Rehabilitation* 11, no. 2 (2026): 129, https://doi.org/10.1007/s41024-026-00804-y.

51. H. A. Mboya, C. K. King'ondu, K. N. Njau, and A. L. Mrema, "Measurement of Pozzolanic Activity Index of Scoria, Pumice, and Rice Husk Ash as Potential Supplementary Cementitious Materials for Portland Cement," *Advances in Civil Engineering* 2017 (2017): 1–13, https://doi.org/10.1155/2017/6952645.

52. J. M. Marangu, M. J. W. Muthengia, and O. J. Kwa-Thiong, "Performance of Potential Pozzolanic Cement in Chloride Media," *IOSR Journal of Applied Chemistry* 7, no. 2 (2014): 36–44.

53. Y. Wang, X. Liu, Z. Xie, H. Wang, W. Zhang, and Y. Xue, "Rapid Evaluation of the Pozzolanic Activity of Bayer Red Mud by a Polymerization Degree Method: Correlations With Alkali Dissolution of (Si+Al) and Strength," *Materials* 14, no. 19 (Sepember 2021): 5546, https://doi.org/10.3390/ma14195546.

54. C. Medina, C. Medina, M. Frías, and S. de, "Design and Characterization of Ternary Cements Containing Rice Husk Ash and Fly Ash," *Construction and Building Materials* 187 (2018): 65–76.

55. S. Sembiring, "Preliminary Study on Functional Groups Characteristics of Asphalt Containing Rice Husk Silica," *Journal of Technomaterials Physics* 1, no. 1 (2019): 61–66, https://doi.org/10.32734/jotp.v1i1.826.

56. D. O. Nduka, B. J. Olawuyi, O. I. Fagbenle, and B. G. Fonteboa, "Assessment of the Durability Dynamics of High-Performance Concrete Blended With a Fibrous Rice Husk Ash," *Crystals* 12, no. 1 (January 2022): 75, https://doi.org/10.3390/cryst12010075.

57. A. S. Malisa and D. H. Chengula, "Study on the Influence of Alkali Activator Solutions on Strength Improvement of Pozzolan Calcium Hydroxide Binders," *Journal of Geoscience and Environment Protection* 10, no. 12 (2022): 313–330, https://doi.org/10.4236/gep.2022.1012018.

58. P. Brzyski, "The Effect of Pozzolan Addition on the Physical and Mechanical Properties of Lime Mortar," *E3S Web of Conferences* 49 (2018): 00009, https://doi.org/10.1051/e3sconf/20184900009.

59. u. İsafça-Kaya, A. Mardani, Y. Kaya, A. Doğangün, and N. Mardani, "Improving Lime-Based Restoration Mortars: Effect of Type and Utilization Rate of Binder and Aggregate," *Materials* 18, no. 5 (2025): 961, https://doi.org/10.3390/ma18050961.

60. A. Allahverdi and J. Ghorbani, "Chemical Activation and Set Acceleration of Lime-Natural Pozzolan Cement," *Ceramics-Silikaty* 50, no. 4 (2006): 193–199.

61. B. Pacewska and I. Wilińska, "Comparative Investigations of Influence of Chemical Admixtures on Pozzolanic and Hydraulic Activities of Fly Ash With the Use of Thermal Analysis and Infrared Spectroscopy," *Journal of Thermal Analysis and Calorimetry* 120, no. 1 (2015): 119–127, https://doi.org/10.1007/s10973-014-4334-x.

62. M. Matinfar and J. A. Nychka, "A Review of Sodium Silicate Solutions: Structure, Gelation, and Syneresis," *Advances in Colloid and Interface Science* 322 (2023): 103036, https://doi.org/10.1016/j.cis.2023.103036.

63. A. M. Rashad, Y. Bai, P. A. M. Basheer, N. B. Milestone, and N. C. Collier, "Hydration and Properties of Sodium Sulfate Activated Slag," *Cement and Concrete Composites* 37 (2013): 20–29, https://doi.org/10.1016/j.cemconcomp.2012.12.010.

64. C. Shi and R. L. Day, "Comparison of Different Methods for Enhancing Reactivity of Pozzolans," *Cement and Concrete Research* 31, no. 5 (2001): 813–818, https://doi.org/10.1016/s0008-8846(01)00481-1.

65. L. Li, A. Darquennes, K. Hannawi, and C. Che, "Effect of the Alkali-Sulphate Activators on the Hydration Process of Blast-Furnace Slag Mortars and Pastes," *Materials* 18, no. 3 (2025): 514, https://doi.org/10.3390/ma18030514.

66. F. Sajedi and H. A. Razak, "The Effect of Chemical Activators on Early Strength of Ordinary Portland Cement-Slag Mortars," *Construction and Building Materials* 24, no. 10 (2010): 1944–1951, https://doi.org/10.1016/j.conbuildmat.2010.04.006.

67. K. H. Khayat and R. W. Day, "Acceleration of the Reactivity of Fly Ash by Chemical Activation," *Cement and Concrete Research* 25, no. 1 (1995): 15–21.

68. I. Wilińska, A. Ostrowski, and B. Pacewska, "Investigation of Different Ways of Activation of Fly Ash–Cement Mixtures," *Journal of Thermal Analysis and Calorimetry* 138, no. 6 (2019): 4203–4213, https://doi.org/10.1007/s10973-019-08485-1.

69. S. Greiser, G. J. G. Gluth, P. Sturm, and C. Jäger, "Correction: Si {Al}, Al{si}, and Al{H} Double-Resonance NMR Spectroscopy Study of Cementitious Sodium Aluminosilicate Gels (Geopolymers) and Gel–Zeolite Composites," *RSC Advances* 13, no. 37 (2023): 26148.

70. Al-S. Khaled, A. A. Adewumi, M. A. Mohd Ariffin, et al., "Acid Resistance of Alkali-Activated Natural Pozzolan and Limestone Powder Mortar," *Sustainability* 14, no. 21 (2022): 14451, https://doi.org/10.3390/su142114451.

71. C. Groot, R. Veiga, I. Papayianni, et al., "RILEM TC 277-LHS Report: Lime-Based Mortars for Restoration–A Review on Long-Term Durability Aspects and Experience From Practice," *Materials and Structures* 55, no. 10 (2022): 245, https://doi.org/10.1617/s11527-022-02052-1.

72. H. S. Gökçe, "Durability of Slag-Based Alkali-Activated Materials: A Critical Review," *Journal of the Australian Ceramic Society* (2024).

73. T. Raghunathan, "Acid Attack on Lime Mortar," *International Journal of Engineering Research and Technology* 11, no. 7 (2022).

Supporting Information

Additional supporting information can be found online in the Supporting Information section. **Supporting Information.** Figure S1. FTIR spectrum of RHA. The spectrum shows a broad O–H stretching band between 3200 and 3600 cm^{-1} attributed to adsorbed moisture and surface hydroxyl groups, an H–O–H bending band at 1637 cm^{-1} corresponding to physically adsorbed water, weak carbonate-related bands at approximately 2063 and 1416 cm^{-1} indicating slight surface carbonation, and silica-related bands at 600, 516, and 424 cm^{-1} assigned to Si–O–Si and Si–O–M vibrations. These features confirm the silica-rich nature of the RHA and support its pozzolanic reactivity. Note: The spectral quality in the 3400–3600 cm^{-1} region was affected by moisture-related instrumental artifacts. Therefore, the exact position and intensity of absorption bands in this region should be interpreted with caution.